nature physics

SUPPLEMENTARY INFORMATION

DOI: 10.1038/NPHYS1639

Calibration of Measurement Errors

The origin of measurement errors in this experiment is understood and the errors vary in a predictable way with parameters and biasing, therefore the errors can be reliably removed using calibration procedures. The two dominant error mechanisms are measurement crosstalk and measurement fidelity. Defining the measurement probabilities P_{AB} of qubits A and B with the column vector $(P_{00}, P_{01}, P_{10}, P_{11})^T$, the intrinsic (actual) probabilities P_i will give measured probabilities P_m according to the matrix equation $P_m = XFP_i$, where X and F are the correction matrices for measurement crosstalk and fidelity, respectively. The order of the matrices reflects the fact that errors in fidelity generate crosstalk (see below). By measuring the correction matrices, the intrinsic probabilities can be calculated from the measured values by the inverted relation $P_i = F^{-1}X^{-1}P_m$.

The procedure for calibrating measurement fidelity for single qubits has been discussed previously[19]. The measurement process, which depends on the $|0\rangle$ qubit state not tunneling and the $|1\rangle$ state tunneling, has small errors from $|0\rangle$ tunneling and $|1\rangle$ not tunneling. Defining f_0 and f_1 as the probabilities to correctly identify the state as $|0\rangle$ and $|1\rangle$, respectively, the measurement fidelity matrix for two qubits is given by

$$F = \begin{pmatrix} f_0 & 1-f_1 \\ 1-f_0 & f_1 \end{pmatrix}_A \otimes \begin{pmatrix} f_0 & 1-f_1 \\ 1-f_0 & f_1 \end{pmatrix}_B$$
$$= \begin{pmatrix} f_{0A}f_{0B} & f_{0A}(1-f_{1B}) & (1-f_{1A})f_{0B} & (1-f_{1A})(1-f_{1B}) \\ f_{0A}(1-f_{0B}) & f_{0A}f_{1B} & (1-f_{1A})(1-f_{0B}) & (1-f_{1A})f_{1B} \\ (1-f_{0A})f_{0B} & (1-f_{0A})(1-f_{1B}) & f_{1A}f_{0B} & f_{1A}(1-f_{1B}) \\ (1-f_{0A})(1-f_{0B}) & (1-f_{0A})f_{1B} & f_{1A}(1-f_{0B}) & f_{1A}f_{1B} \end{pmatrix},$$

where $\otimes$ is the tensor product. We measure these fidelities by biasing only one qubit into operation, and then measuring the tunneling probabilities for the $|0\rangle$ and $|1\rangle$ states, with the latter produced by a microwave π-pulse optimized for the largest tunneling probability. This

 DOI: 10.1038/NPHYS1639

calibration depends on accurately producing the $|1\rangle$ state, which we have demonstrated can be done with 98% accuracy[20]. The 2% error arises from T_1 energy decay, which can be measured and corrected for in the calibration.

Measurement crosstalk for two capacitively coupled Josephson phase qubits has been studied and understood in previous work[18]. The crosstalk mechanism arises from the release of energy when one qubit tunnels, which then excites the second qubit and increases its probability to tunnel. For this mechanism, crosstalk contributes when one qubit state is measured as 1, causing the other qubit state, when in the 0 state, to have probability x to be excited and thus measured in the 1 state. The matrix describing measurement crosstalk for both qubits is thus

$$X = \begin{pmatrix} 1 & 0 & 0 & 0 \\ 0 & 1-x_{BA} & 0 & 0 \\ 0 & 0 & 1-x_{AB} & 0 \\ 0 & x_{BA} & x_{AB} & 1 \end{pmatrix},$$

where x_{AB} (x_{BA}) is the probability of the $|1\rangle$ state of qubit A (qubit B) exciting a $|0\rangle \rightarrow |1\rangle$ transition on qubit B (qubit A).

The two unknowns in the X matrix can be directly determined from the 3 independent equations in $P_m = X(FP_i)$, where FP_i is obtained from the F matrix calibration procedure described above.

A more robust method is to compare the differences in tunneling of the first qubit caused by a change in tunneling of the second. From the four measurement probabilities P_{00}, P_{01}, P_{10}, and P_{11}, we extract for each qubit independent probabilities to be in the $|1\rangle$ state by "tracing out" the other qubit

$$P_{1\mathrm{A}} \equiv P_{10} + P_{11}$$

$$P_{1\mathrm{B}} \equiv \mathrm{P}_{01} + P_{11}$$

We measure $P_{1\mathrm{A}}(00)$ and $P_{1\mathrm{B}}(01)$ for the two cases where we prepare the initial states $|00\rangle$ and $|01\rangle$, respectively. Using the correction matrices for X and F, we calculate

$$\begin{aligned} \frac{P_{1A}(01) - P_{1A}(00)}{P_{1B}(01) - P_{1B}(00)} &= \frac{f_{0A}}{1-(1-f_{0A})x_{AB}} x_{BA} , \\ &\cong f_{0A} x_{BA} \end{aligned}$$

where the approximate result arises from both correction terms in the denominator, $1-f_{0A}$ and x_{BA}, being small. This result holds even if the states $|00\rangle$ and $|01\rangle$ are not prepared perfectly, as we calculate the ratio of the change in probabilities. A similar result for $f_{0B}x_{AB}$ is obtained for the initial states $|00\rangle$ and $|10\rangle$.

We also perform a consistency check on the measurements of x_{AB} and x_{BA} for the simple case of measuring only the $|00\rangle$ state when $f_{0A}, f_{0B} \neq 0$. Here, a general solution is not possible as there are four unknowns f_{0A}, f_{0B}, x_{AB}, and x_{BA} and only three equations for the probabilities. However, by assuming a fixed ratio between the two crosstalk parameters $k = x_{BA}/x_{AB}$, a solution can be found:

$$x_{AB} = \frac{P_{00} + kP_{00} - k + kP_{10} + P_{01} - 1 - \sqrt{((1-P_{00}-P_{01}) - k(1-P_{00}-P_{10}))^2 + 4kP_{10}P_{01}/P_{00}}}{2k(P_{00}-1)}$$

For the device measured here, we found measurement fidelities that were near unity: $f_{0A} = 0.95$ and $f_{1A} = 0.95$ for qubit A, and $f_{0B} = 0.93$ and $f_{1B} = 0.93$ for qubit B. Crosstalk was measured to be $x_{AB} = x_{BA} = 0.117$.

Physicality of the χ Matrix

We define the original χ matrix data as χ_e, and the data with measurement effects calibrated out as χ_m. Plots of χ_e and χ_m are shown in Supplementary Figures 1 and 2 respectively; some negative eigenvalues are found for this data, which implies it is unphysical. To be physical, the experimentally obtained χ matrix must be positive and trace preserving. The closest physical estimates to these matrices given these constraints are χ_e^p and χ_m^p, as shown in Supplementary Figure 3 and in the Figure 4 of the main paper, respectively.

To perform the physical estimation, we used the MATLAB packages YALMIP and SeDuMi to perform a semidefinite programming convex optimization. As in reference 24, we then histogrammed the differences Δ_p between the peak heights of χ_e and χ_e^p for the real parts of each of the 256 matrix elements. We fit a Gaussian, $\gamma\exp(-\Delta^2/\sigma^2)$ to the histogram and obtained a sense of the relative error of the process tomography from its width

 DOI: 10.1038/NPHYS1639

σ. We repeated this procedure also for χ_m^p, and plotted these histograms and fits for χ_m^p and χ_e^p as shown in Supplementary Figures 4a and 4b.

The fidelities of the above mentioned χ matrices are: $Tr(\chi_t\,\chi_e^p)$ =0.49, $Tr(\chi_t\,\chi_m^p)$ =0.61, $Tr(\chi_t\,\chi_e)$ =0.51, $Tr(\chi_t\,\chi_m)$ =0.65.

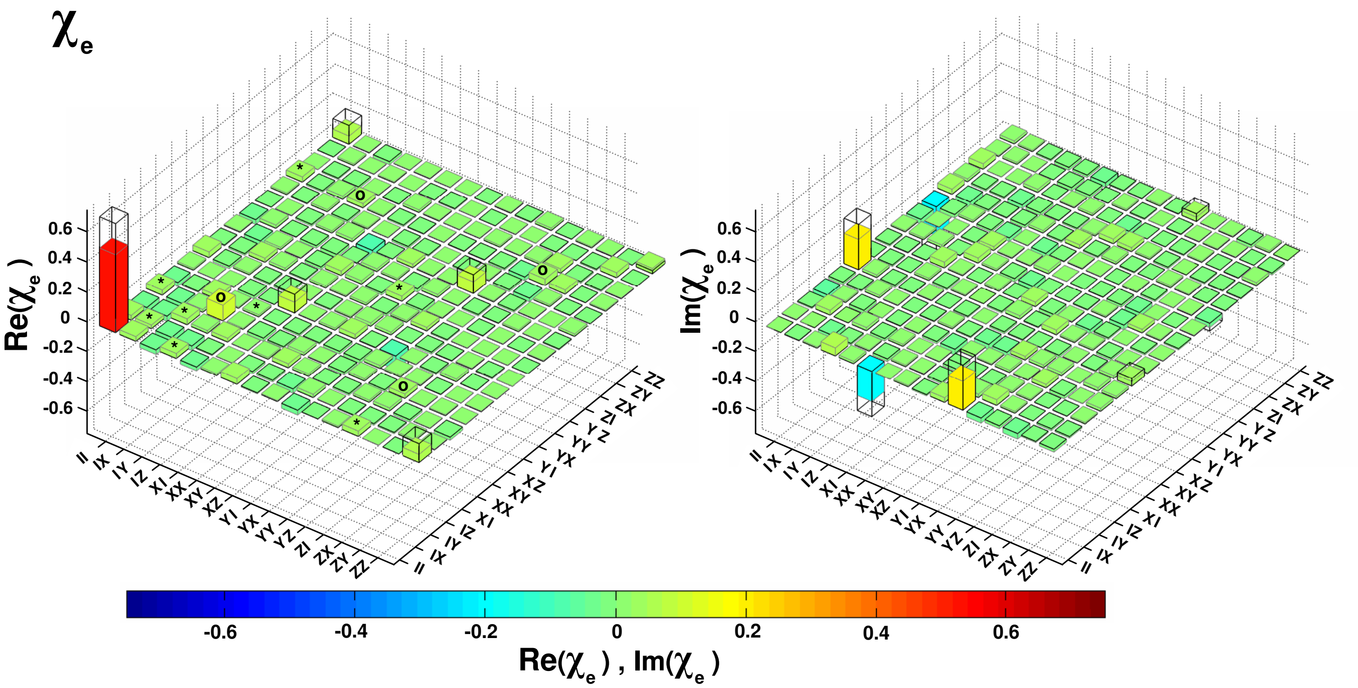
χ_e
Re(χ_e)
Im(χ_e)
Re(χ_e) , Im(χ_e)
-0.6
-0.4
-0.2
0
0.2
0.4
0.6

DOI: 10.1038/NPHYS1639

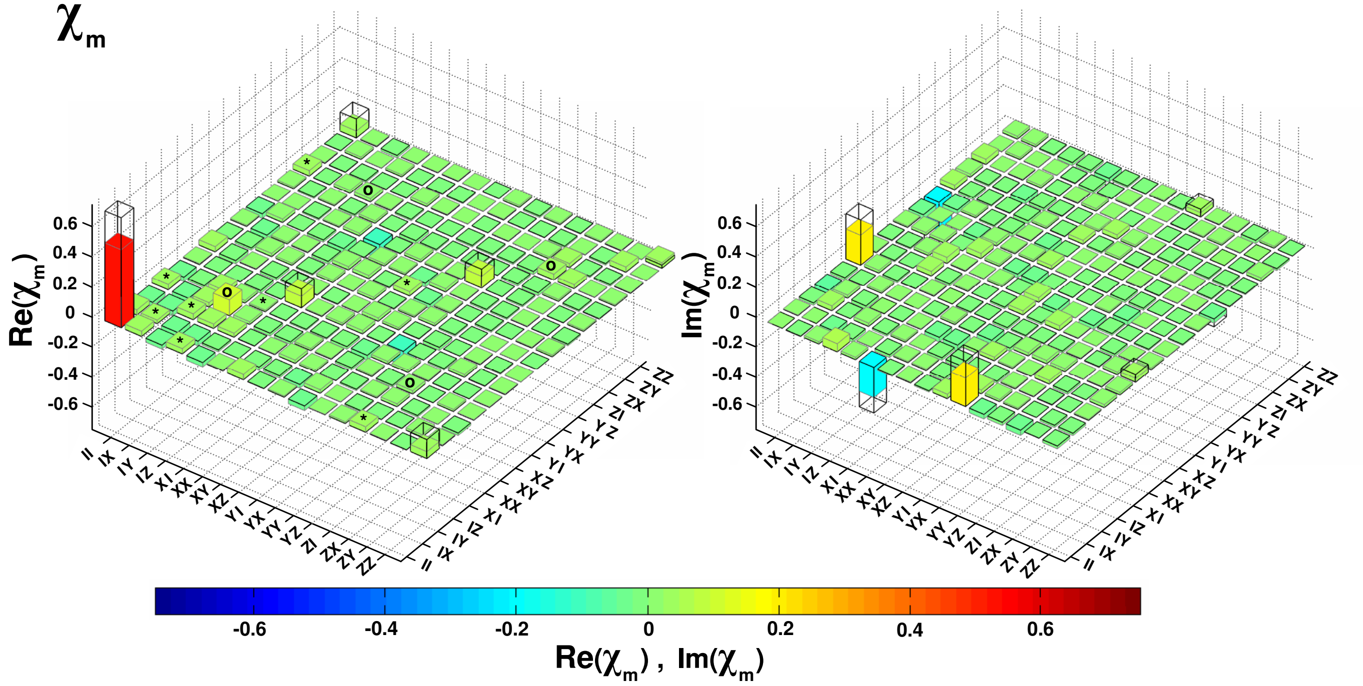

DOI: 10.1038/NPHYS1639

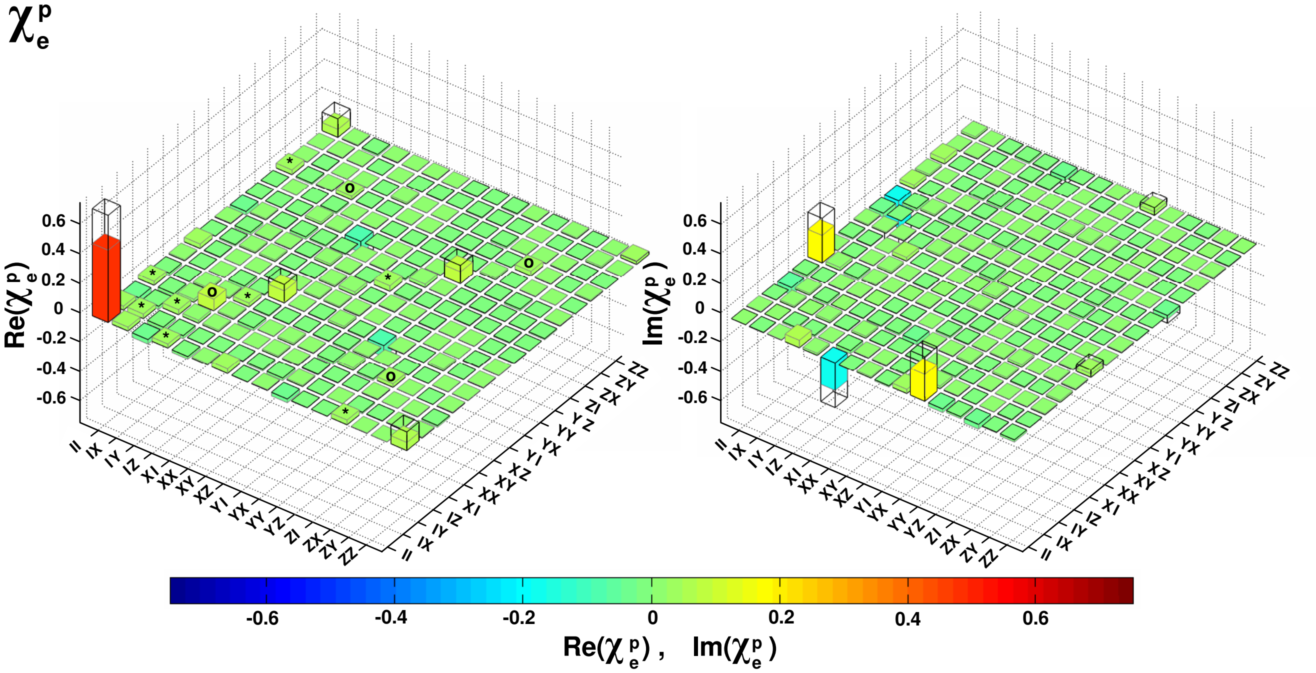

DOI: 10.1038/NPHYS1639